

One-dimensional tunable ferroelectric photonic crystals based on $\text{Ba}_{0.7}\text{Sr}_{0.3}\text{TiO}_3/\text{MgO}$ multilayer thin films

K. L. Jim,^{a)} D. Y. Wang, C. W. Leung, C. L. Choy, and H. L. W. Chan

Department of Applied Physics and Materials Research Centre, The Hong Kong Polytechnic University, Hung Hom, Kowloon, Hong Kong, China

(Received 1 December 2007; accepted 14 February 2008; published online 21 April 2008)

Tunable photonic crystals (PCs) have attracted much attention in the past decade because of their various applications, such as ultrafast optical filters and optical waveguides with add-drop functionalities. One way of achieving tunability is to make use of ferroelectric materials since the refractive index of ferroelectric materials can be electrically tuned through the electro-optic effect. In this paper, we present our work on developing a tunable one-dimensional (1D) PC based on a $\text{Ba}_{0.7}\text{Sr}_{0.3}\text{TiO}_3/\text{MgO}$ multilayer structure. The photonic band structures and band gap maps of the PC were calculated by using the plane-wave expansion (PWE) method. It is found that the gap center linearly shifts with the change in the refractive index of $\text{Ba}_{0.7}\text{Sr}_{0.3}\text{TiO}_3$. A ferroelectric 1D PC consisting of a $\text{Ba}_{0.7}\text{Sr}_{0.3}\text{TiO}_3/\text{MgO}$ multilayer thin film was epitaxially deposited on a MgO (001) single-crystal substrate by pulsed laser deposition. A photonic band gap in the visible region is observed in the transmission spectrum of the multilayer thin film. The center wavelength of the band gap is ~ 464 nm, which agrees with the simulation results obtained by the transfer matrix method. The band gap can be tuned by applying an electric field E . The band gap shifts by about 2 nm when the thin film is subjected to a dc voltage of 240 V ($E \sim 12$ MV/m). This shift corresponds to an $\sim 0.5\%$ change in the refractive index of the $\text{Ba}_{0.7}\text{Sr}_{0.3}\text{TiO}_3$ layer, as calculated by the PWE method. © 2008 American Institute of Physics. [DOI: [10.1063/1.2907418](https://doi.org/10.1063/1.2907418)]

I. INTRODUCTION

Over the past decade, there has been great interest in photonic crystals (PCs) due to their ability to manipulate photons and potential applications in photonics information technology.^{1–5} PCs represent a special class of structured materials, in which the dielectric constant exhibits spatially periodic modulations. With different combinations of materials and configurations, PCs exhibit different photonic band structures and photonic band gaps (PBGs). Light waves with frequencies lying within a PBG cannot propagate inside PCs, and there are often anisotropic dispersions at frequencies near a PBG.

The properties of PCs depend on the configuration of the constituent materials, which cannot be modified after fabrication. On the other hand, photonic band structures are also dependent on the refractive indices of the constituent materials. If the photonic band structures of the PCs can be externally modulated by some other means, the PCs may be applicable as active optical devices. Indeed, many schemes have been proposed to realize the tunability of PCs by external parameters, such as electric field, magnetic field, temperature, and strain.^{6–9} Different tuning mechanisms have their own benefits in various applications. Recently, fast-response tunable PC filters^{10–12} have attracted much attention due to their important applications in chip-to-chip and on-chip optical communications. For such applications, it is ad-

vantageous to achieve tunability through the electro-optic (EO) effect, for which the intrinsic response speed is known to be in the gigahertz range.^{13,14}

The EO effect is one of the interesting characteristics of ferroelectric materials. The refractive index of a ferroelectric material can be modulated by applying an external electric field. Therefore, it is expected that index-tunable PCs can be realized if one fabricates PCs by using ferroelectric materials. Great efforts have been made in recent years to develop PCs based on lanthanum modified lead zirconate titanate (PLZT). Since PLZT has a high transparency and excellent EO properties, it is a good material candidate for tunable PC fabrication. PCs with different geometries based on PLZT thin films have been reported, including two-dimensional (2D) and three-dimensional (inverse opal) PCs.^{15–17} However, lead-containing materials are environmentally hazardous. Therefore, a lead-free material, such as barium strontium titanate (BST), is an attractive alternative to be used for making one-dimensional (1D) tunable PC filters.

BST is considered to be a promising EO material since the discovery of a high EO coefficient in BST thin films.¹⁸ In our previous studies, $\text{Ba}_{0.7}\text{Sr}_{0.3}\text{TiO}_3$ thin films epitaxially grown on single-crystal substrates showed low optical losses and good EO performances, indicating their potential uses in active optical devices.^{19,20} Many recent works focused on self-assembled PC structures, such as colloidal crystals and inverse opal structures.^{17,21} Both of these structures have limited tunability and the fabrication processes are relatively complicated. In comparison, periodic multilayer structures (1D PC) have many advantages in terms of material proper-

^{a)} Author to whom correspondence should be addressed. Electronic mail: jim.kl@polyu.edu.hk.

ties, processability,^{22,23} as well as cost.²⁴ Moreover, it is possible to fabricate large-area PCs by using multilayer structures.

In this paper, we show that a PC based on a Ba_{0.7}Sr_{0.3}TiO₃/MgO multilayer thin film, which is active in the visible spectrum, can be easily produced. In Sec. II, we will briefly review the plane-wave expansion (PWE) method and the transfer matrix method (TMM) for the calculations of the photonic band structure and transmission spectrum of a PC structure, respectively. The shifts in band gaps with the change in the refractive index of Ba_{0.7}Sr_{0.3}TiO₃, as calculated by the PWE method, will be given in Sec. III. Finally, the fabrication details of a 1D PC composed of a Ba_{0.7}Sr_{0.3}TiO₃/MgO multilayer thin film and its characterization will be discussed in Secs. IV and V, respectively.

II. PLANE-WAVE EXPANSION AND TRANSFER MATRIX METHODS

A. Plane-wave expansion method

The band structure of PCs can be calculated by using the PWE method.²⁵ The Maxwell equations for electromagnetic (EM) waves in a system with a periodic distribution of dielectric constants can be simplified to

$$\nabla \times \left(\frac{1}{\varepsilon(r)} \nabla \times H \right) = \frac{\omega^2}{c^2} H. \quad (1)$$

Here, $\varepsilon(r)$ is the position-dependent dielectric function, H is the magnetic field, ω is the frequency, and c is the speed of light in vacuum. Because the system is periodic, the dielectric function and the H field can be expanded in terms of plane waves:

$$\frac{1}{\varepsilon(r)} = \sum_g \varepsilon_g^{-1} e^{ig \cdot r}, \quad (2a)$$

$$M = \begin{pmatrix} \cos(k_0 n d \cos \psi) & -\frac{i}{n \cos \psi} \sin(k_0 n d \cos \psi) \\ -i n \cos \psi \sin(k_0 n d \cos \psi) & \cos(k_0 n d \cos \psi) \end{pmatrix} \quad \text{for TE polarization,} \quad (5)$$

where k is the wavevector of the EM wave, ψ is the angle between k and the normal of the film, and n and d are the refractive index and the thickness of the film, respectively. The transfer matrix of a multilayer film ($M_{\text{multilayer}}$) consisting of N layers is obtained by multiplication of the transfer matrices of the layers:

$$M_{\text{multilayer}} = \begin{pmatrix} m_{11} & m_{12} \\ m_{21} & m_{22} \end{pmatrix} = \prod_{j=1}^N M_j(n_j, d_j). \quad (6)$$

The transmission coefficient (t) and the transmittance (T) are then given by

$$H(r) = \sum_g H_g e^{i(k+g) \cdot r}, \quad (2b)$$

where k is the wavevector and g is the reciprocal lattice vector. Both vectors are in units of $2\pi/a$, where a is the period of the PC. For the propagation of light along the normal (z) direction of a 1D PC composed of alternative layers of dielectric materials (ε_1 and ε_2), the transverse electric (TE) mode and the transverse magnetic (TM) mode are degenerate.

Combining Eqs. (1), (2a), and (2b), we obtain the following matrix equation:

$$\sum_{g'} |k+g\rangle |k+g'\rangle \varepsilon_{g-g'}^{-1} H_{g'} = \Omega^2 H_g, \quad (3)$$

where

$$\varepsilon_{g-g'}^{-1} = \begin{cases} \frac{1}{\varepsilon_1} f + \frac{1}{\varepsilon_2} (1-f) & \text{for } g=0 \\ \left(\frac{1}{\varepsilon_1} - \frac{1}{\varepsilon_2} \right) f \frac{\sin(g\pi f)}{g\pi f} & \text{for } g \neq 0 \end{cases}, \quad (4)$$

where $\Omega = \omega a / 2\pi c$ is the normalized frequency and f is the filling (volume) fraction of material 1. The band structure of the 1D PC (Ω against k) is then obtained by solving the eigenvalue equation [Eq. (3)].

B. Transfer matrix method

The TMM (Ref. 26) utilizes the transfer (characteristic) matrix to describe the propagation of EM waves inside a single homogeneous film, including the interfacial effects. By knowing the propagation details of the EM waves inside a system, it is straightforward to obtain the transmission spectrum of that system. The transfer matrix of a homogeneous film is given by

$$t = \frac{2n_i \cos \psi_i}{(m_{11} + m_{12} n_S \cos \psi_S) n_i \cos \psi_i + m_{21} + m_{22} n_S \cos \psi_S}, \quad (7)$$

and

$$T = \frac{\text{Re}(n_S \cos \psi_S)}{\text{Re}(n_i \cos \psi_i)} |t|^2, \quad (8)$$

where i and S denote the first (incident) layer and the last (substrate) layer, respectively. The transfer matrices and the expressions of transmission and transmittance for TM polarization can be found in Ref. 26.

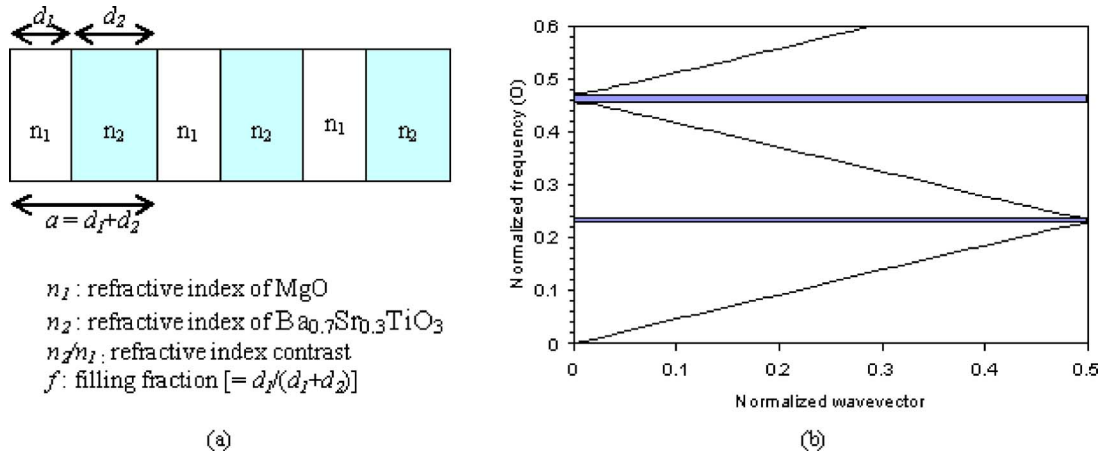


FIG. 1. (Color online) (a) Schematic of a typical 1D PC. (b) band structure of a $\text{Ba}_{0.7}\text{Sr}_{0.3}\text{TiO}_3/\text{MgO}$ 1D PC with a filling fraction of 0.1. The shaded areas show the PBGs.

III. NUMERICAL CALCULATION

The schematic of a typical 1D PC is shown in Fig. 1(a). 1D PCs are characterized by the refractive index contrast and the filling fraction. The refractive index contrast is the ratio of the higher refractive index to the lower refractive index (n_2/n_1) in the multilayer system. The filling fraction f is the ratio between the thickness of the lower refractive index layer (the MgO layer in the present case) and the period of the PC, i.e., $f = d_1/(d_1 + d_2)$. The band structure of a $\text{Ba}_{0.7}\text{Sr}_{0.3}\text{TiO}_3/\text{MgO}$ 1D PC calculated by the PWE method is given in Fig. 1(b) as an example. The refractive indices of $\text{Ba}_{0.7}\text{Sr}_{0.3}\text{TiO}_3$ and MgO are taken to be 2.2 and 1.73, respectively. The filling fraction is set to 0.1. The vertical axis represents the normalized frequency, $\Omega = \omega a / 2\pi c = a/\lambda$, where a is the period of the 1D PC and λ is the wavelength. The horizontal axis represents the k point along the symmetry direction of the first Brillouin zone. The shaded areas illustrate the PBGs. Normally, the PBGs are wider if the refractive index contrast is larger. The photonic band structures of the 1D PC in this work were calculated by using 71 plane waves such that the normalized frequencies converged to within 10^{-4} .

In order to examine how a change in the refractive index of $\text{Ba}_{0.7}\text{Sr}_{0.3}\text{TiO}_3$ affects the PBG of the 1D PC, gap maps of the first gap in the $\text{Ba}_{0.7}\text{Sr}_{0.3}\text{TiO}_3/\text{MgO}$ 1D PC with different percentage changes in the refractive index of $\text{Ba}_{0.7}\text{Sr}_{0.3}\text{TiO}_3$ were calculated. The results are shown in Fig. 2. It can be seen from Fig. 2 that when the refractive index of $\text{Ba}_{0.7}\text{Sr}_{0.3}\text{TiO}_3$ (n_{BST}) increases, the gaps shift to lower frequencies. Moreover, the magnitudes of the gap shift weakly depend on the filling fraction for $f = 0 - 0.4$. In the fabrication of $\text{Ba}_{0.7}\text{Sr}_{0.3}\text{TiO}_3/\text{MgO}$ 1D PC by the pulsed laser deposition (PLD) technique, it is more convenient to prepare samples with a lower filling fraction (i.e., with a thinner MgO layer) because the deposition rate of MgO is much lower than that of $\text{Ba}_{0.7}\text{Sr}_{0.3}\text{TiO}_3$. Thus, we concentrate our work on $f = 0.1$.

IV. EXPERIMENTAL

The PLD technique was employed to prepare a 1D PC consisting of an epitaxial $\text{Ba}_{0.7}\text{Sr}_{0.3}\text{TiO}_3/\text{MgO}$ multilayer

thin film. Alternate layers of $\text{Ba}_{0.7}\text{Sr}_{0.3}\text{TiO}_3$ and MgO were deposited on MgO (001) single-crystal substrates by irradiating stoichiometric targets with a laser beam with a 248 nm wavelength and a 25 ns pulse duration from a KrF excimer laser (Lambda Physik COMPex 250). The pulse energies of the laser beam were 250 and 350 mJ for the deposition of the $\text{Ba}_{0.7}\text{Sr}_{0.3}\text{TiO}_3$ and MgO layers, respectively, and the repetition rate was 10 Hz. The distance between the target and the substrate was fixed to 50 mm. The substrate temperature was maintained at 750 °C. The oxygen partial pressure was kept at 27 Pa during the laser ablation process. The deposition rates for $\text{Ba}_{0.7}\text{Sr}_{0.3}\text{TiO}_3$ and MgO were found to be about 20 and 5 nm/min, respectively. The fabricated 1D PC has five periods, with each period consisting of an ~ 90 nm thick $\text{Ba}_{0.7}\text{Sr}_{0.3}\text{TiO}_3$ layer and an ~ 10 nm thick MgO layer. After deposition, the PC was postannealed at 1000 °C in a tube furnace for 3 h. The crystal structure of the $\text{Ba}_{0.7}\text{Sr}_{0.3}\text{TiO}_3/\text{MgO}$ multilayer thin film was examined by using an x-ray diffractometer (XRD) (Bruker D8 Discover) equipped with Cu $K\alpha$ radiation.

The optical transmission spectrum of the $\text{Ba}_{0.7}\text{Sr}_{0.3}\text{TiO}_3/\text{MgO}$ multilayer thin film was measured by using a PerkinElmer Lambda 18 UV-visible spectrometer.

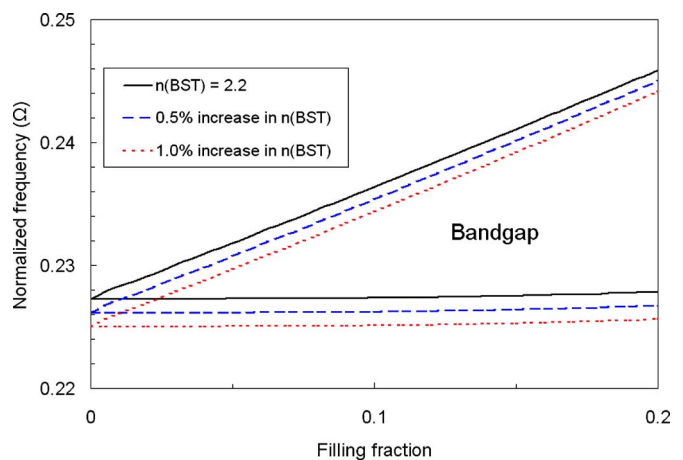


FIG. 2. (Color online) Gap maps of the first gap of a $\text{Ba}_{0.7}\text{Sr}_{0.3}\text{TiO}_3/\text{MgO}$ 1D PC for different changes in the refractive index of $\text{Ba}_{0.7}\text{Sr}_{0.3}\text{TiO}_3$.

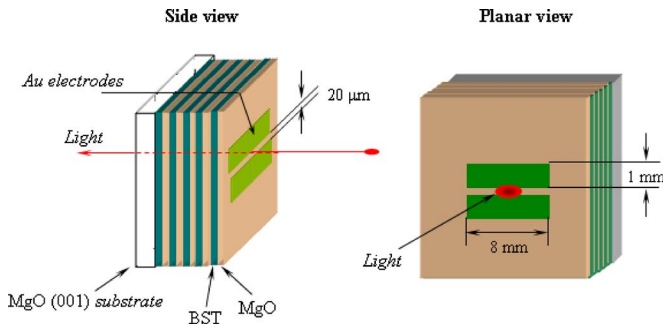


FIG. 3. (Color online) Schematic showing the experiment for observing the PBG shift of the $\text{Ba}_{0.7}\text{Sr}_{0.3}\text{TiO}_3/\text{MgO}$ multilayer thin film.

The electrode configuration used for applying an electric field consisted of two coplanar electrodes with dimensions of $1.0 \times 8.0 \text{ mm}^2$ and separated by a $20 \mu\text{m}$ wide gap (see Fig. 3).

V. RESULTS AND DISCUSSION

Figure 4 shows the $\theta/2\theta$ XRD pattern of the $\text{Ba}_{0.7}\text{Sr}_{0.3}\text{TiO}_3/\text{MgO}$ multilayer thin film. Only (00 l) peaks of the $\text{Ba}_{0.7}\text{Sr}_{0.3}\text{TiO}_3$ layers appear in the XRD patterns, indicating that the $\text{Ba}_{0.7}\text{Sr}_{0.3}\text{TiO}_3$ layers have a pure perovskite phase. It is believed that the diffraction peaks of the MgO layers are submerged in the peaks of the MgO single-crystal substrate, so no peaks of the MgO layers can be observed. Rocking curve measurements of the $\text{Ba}_{0.7}\text{Sr}_{0.3}\text{TiO}_3$ (002) reflections revealed that the full width at half maximum is about 0.53° , which indicates that the crystallites are of high quality. The in-plane alignment of the $\text{Ba}_{0.7}\text{Sr}_{0.3}\text{TiO}_3$ thin films with respect to the major axes of the (001) substrates was confirmed by the XRD off-axis φ scan of the $\text{Ba}_{0.7}\text{Sr}_{0.3}\text{TiO}_3$ (202) and MgO (202) reflections, as shown in the inset of Fig. 4, indicating epitaxial growth of the $\text{Ba}_{0.7}\text{Sr}_{0.3}\text{TiO}_3$ layers. The losses in optical devices originate from various structural defects, such as point defects, grain boundaries, misorientation, and surface roughness. Hence,

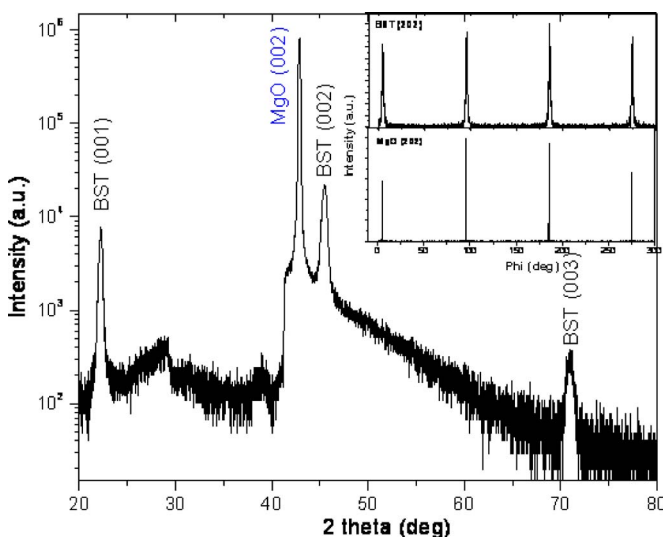


FIG. 4. (Color online) XRD $\theta/2\theta$ scan of the $\text{Ba}_{0.7}\text{Sr}_{0.3}\text{TiO}_3/\text{MgO}$ multilayer thin film. The inset shows the φ scan of the $\text{Ba}_{0.7}\text{Sr}_{0.3}\text{TiO}_3$ (202) and substrate (202) reflections.

fabrication of defect-free films, such as epitaxial single-crystalline thin films, is required for optical device applications.

The transmission spectrum of the $\text{Ba}_{0.7}\text{Sr}_{0.3}\text{TiO}_3/\text{MgO}$ multilayer thin film is shown in Fig. 5(a). The transparency of the multilayer film sharply drops in the UV region and the absorption edge (threshold wavelength) is located at 318 nm, which is quite close to that of a single $\text{Ba}_{0.7}\text{Sr}_{0.3}\text{TiO}_3$ thin film grown on a MgO (001) substrate.¹⁹ A PBG (transmission dip) with a center wavelength of $\sim 464 \text{ nm}$ is observed in the spectrum. In order to confirm that the transmission dip is not caused by the intrinsic absorption of the perovskite phase of $\text{Ba}_{0.7}\text{Sr}_{0.3}\text{TiO}_3$, a $\text{Ba}_{0.7}\text{Sr}_{0.3}\text{TiO}_3$ thin film of $\sim 300 \text{ nm}$ thickness was deposited on a MgO (001) substrate under the same conditions. The transmission spectrum of the $\text{Ba}_{0.7}\text{Sr}_{0.3}\text{TiO}_3$ thin film was measured and is shown in the inset of Fig. 5(a). The film is highly transparent in the visible region and does not show any absorption. A theoretical calculation of the transmission spectrum of the $\text{Ba}_{0.7}\text{Sr}_{0.3}\text{TiO}_3/\text{MgO}$ multilayer thin film was conducted by using the TMM. The complex refractive index profile of the $\text{Ba}_{0.7}\text{Sr}_{0.3}\text{TiO}_3$ used for the TMM calculation, which is shown in the inset of Fig. 5(b), was obtained by the single Tauc-Lorentz dispersion formula.²⁷ As shown in Fig. 5(b), a transmission dip, which corresponds to a PBG, occurs at $\sim 464 \text{ nm}$ in the calculated spectrum. The general features of the calculated spectrum above the absorption edge agree very well with the experimental result. Figure 6 shows that the dip occurs at $\sim 450 \text{ nm}$ for a $\text{Ba}_{0.7}\text{Sr}_{0.3}\text{TiO}_3/\text{MgO}$ 1D PC with different numbers of periods (N). As the number of periods increases, the dips become deeper, demonstrating that a 1D PC with a larger number of periods exhibits a better filtering function. To achieve a transmittance of 0.5, which corresponds to -3 dB , nine periods of $\text{Ba}_{0.7}\text{Sr}_{0.3}\text{TiO}_3/\text{MgO}$ are required.

Figure 7 shows the shift in the transmission spectrum when a dc voltage of 240 V (corresponding to an electric field of about 12 MV/m) is applied. With an increase in the applied voltage, the band gap (dip) at $\sim 464 \text{ nm}$ slightly shifts ($\sim 2 \text{ nm}$) to a longer wavelength. The EO effect could be the origin of the band gap tunable phenomenon since the refractive index of a ferroelectric material changes when it is subjected to an external electric field. In our previous works,^{19,20} we showed that $\text{Ba}_{0.7}\text{Sr}_{0.3}\text{TiO}_3$ thin films have good EO properties. Thus, it is reasonable that the band gap is shifted when an electric field is applied to the $\text{Ba}_{0.7}\text{Sr}_{0.3}\text{TiO}_3/\text{MgO}$ multilayer thin film.

The shift in the gap center in a $\text{Ba}_{0.7}\text{Sr}_{0.3}\text{TiO}_3/\text{MgO}$ 1D PC for different percentage changes in the refractive index of $\text{Ba}_{0.7}\text{Sr}_{0.3}\text{TiO}_3$ was calculated by using the PWE method and is shown in Fig. 8. It is seen that the gap center linearly shifts with the change in the refractive index of $\text{Ba}_{0.7}\text{Sr}_{0.3}\text{TiO}_3$. A 2 nm shift of the gap center corresponds to an $\sim 0.5\%$ change in n_{BST} . Therefore, our experimental result indicates that the electric field induced change in the refractive index of $\text{Ba}_{0.7}\text{Sr}_{0.3}\text{TiO}_3$ is about 0.5%, which is comparable to that of (Pb,La)TiO₃ thin films.²⁸ Since the band gap of the $\text{Ba}_{0.7}\text{Sr}_{0.3}\text{TiO}_3/\text{MgO}$ 1D PC can be electrically modulated, the BST-based 1D PCs are potential candidates in developing

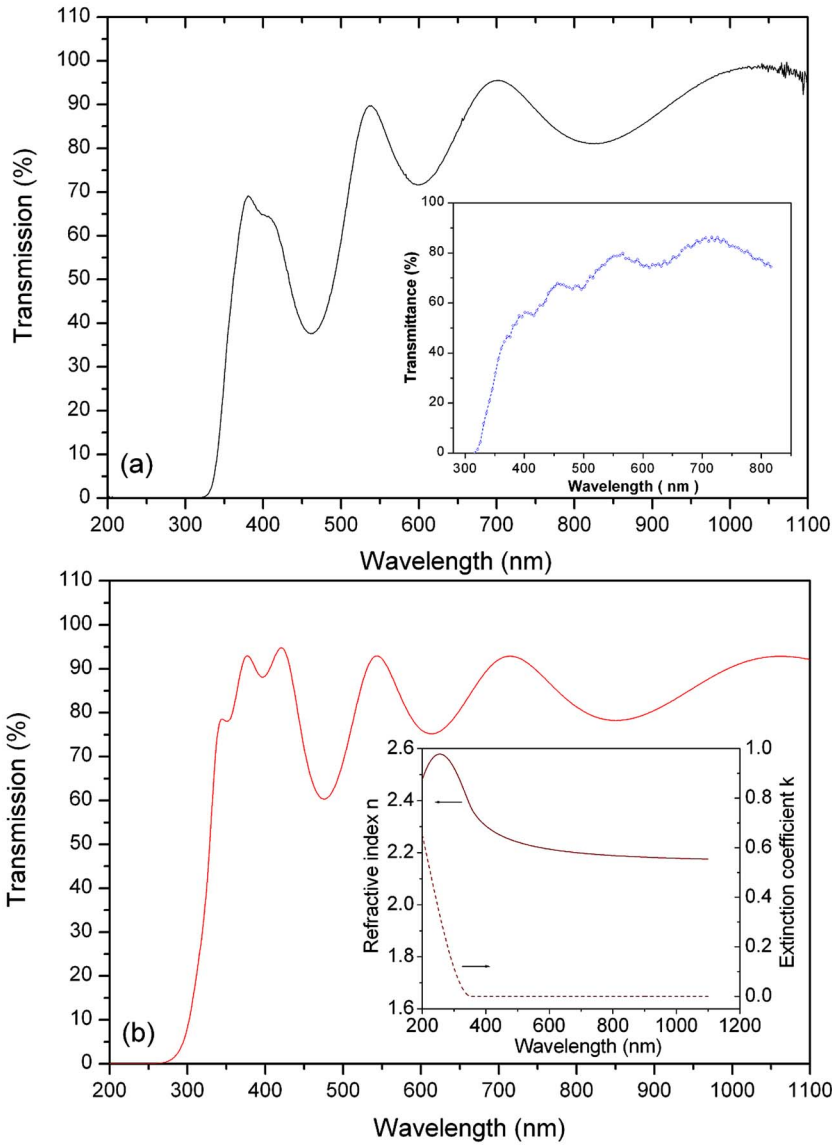


FIG. 5. (Color online) (a) Observed transmission spectrum of the $Ba_{0.7}Sr_{0.3}TiO_3/MgO$ multilayer thin film. The inset shows the transmission spectrum of the $Ba_{0.7}Sr_{0.3}TiO_3$ thin film grown on a $MgO(001)$ substrate. (b) Calculated transmission spectrum of the $Ba_{0.7}Sr_{0.3}TiO_3/MgO$ multilayer thin film with five periods. The inset shows the complex refractive index profile of the $Ba_{0.7}Sr_{0.3}TiO_3$ used for the calculation.

fast-response tunable optical filters because the intrinsic response speed of the EO effect is known to be in the gigahertz range. Besides considering the 1D PC structures, it is expected that the 2D PC structures composed of the EO mate-

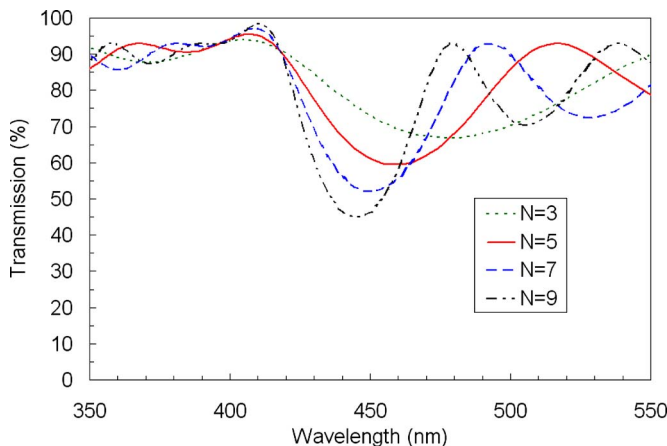


FIG. 6. (Color online) Calculated transmission spectrum of the $Ba_{0.7}Sr_{0.3}TiO_3/MgO$ multilayer thin films with different numbers of periods (N).

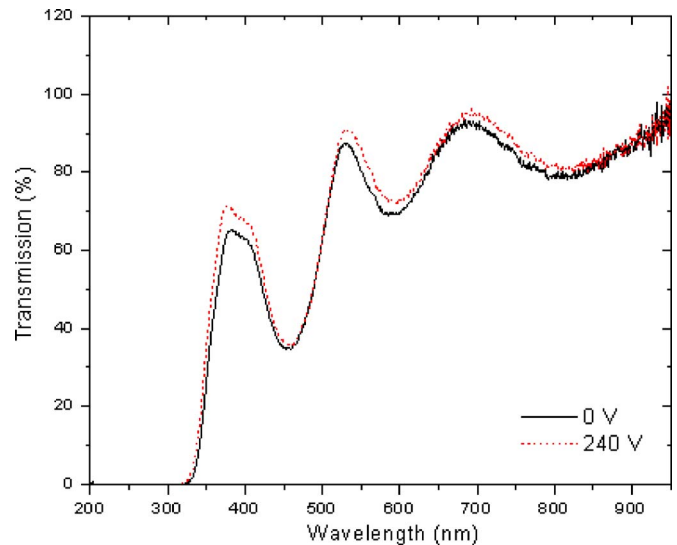


FIG. 7. (Color online) Measured transmission spectrum of the $Ba_{0.7}Sr_{0.3}TiO_3/MgO$ multilayer thin film with (dotted curve) and without (solid curve) the application of a dc voltage of 240 V.

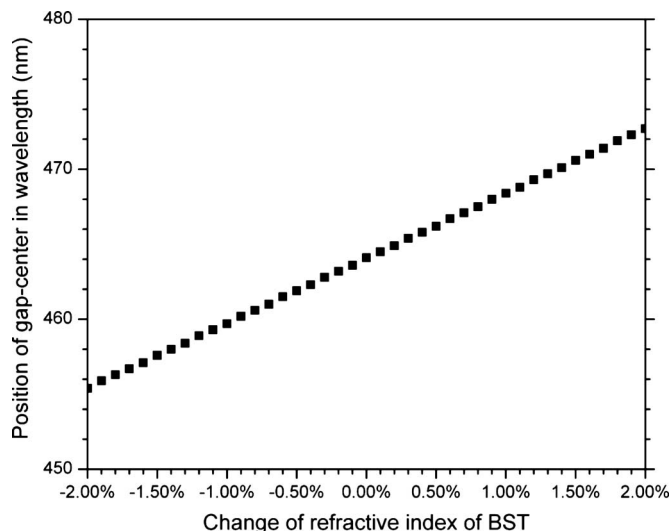


FIG. 8. Position of the gap center of a $\text{Ba}_{0.7}\text{Sr}_{0.3}\text{TiO}_3/\text{MgO}$ 1D PC ($f=0.1$) for different percentage changes in the refractive index of $\text{Ba}_{0.7}\text{Sr}_{0.3}\text{TiO}_3$.

rials would show even more functionalities. It has been demonstrated that 2D PCs composed of EO materials can be used to develop devices with tunable negative refraction²⁹ and a PC slab waveguide resonator with sub-1-V sensitivity.³⁰ It is believed that BST is a promising lead-free ferroelectric material in developing PC devices.

VI. CONCLUSIONS

In this paper, we investigated the tunability of the PBG of a $\text{Ba}_{0.7}\text{Sr}_{0.3}\text{TiO}_3/\text{MgO}$ 1D PC arising from the EO effect. The relationship between the shift in the band gap and the change in the refractive index of $\text{Ba}_{0.7}\text{Sr}_{0.3}\text{TiO}_3$ was examined by using the PWE method. It is found that the gap center linearly shifts with the change in the refractive index of $\text{Ba}_{0.7}\text{Sr}_{0.3}\text{TiO}_3$. A ferroelectric 1D PC consisting of five layers of $\text{Ba}_{0.7}\text{Sr}_{0.3}\text{TiO}_3$ and five layers of MgO alternatively deposited on a MgO substrate was successfully fabricated by PLD. XRD reveals that all the layers were epitaxially grown on the MgO (001) single-crystal substrate. A PBG at ~ 464 nm was observed in the transmission spectrum, which agrees well with the theoretical calculation by the TMM. It is observed that the PBG of the multilayer film can be tuned by an external electric field E . The band gap shifts by about 2 nm when the PC is subjected to a dc voltage of 240 V ($E \sim 12$ MV/m). This shift corresponds to a 0.5% change in the refractive index of $\text{Ba}_{0.7}\text{Sr}_{0.3}\text{TiO}_3$ according to the calculation by the PWE method.

ACKNOWLEDGMENTS

This work was supported by the Center for Smart Materials of the Hong Kong Polytechnic University and PolyU

Research Grant Nos. 1-BBZ3 and 1-BB95. Financial support from Hong Kong Polytechnic University Internal Grant No. 1-BB9P is also acknowledged.

- ¹A. Mekis, J. C. Chen, I. Kurland, S. Fan, P. R. Villeneuve, and J. D. Joannopoulos, *Phys. Rev. Lett.* **77**, 3787 (1996).
- ²E. Chow, S. Y. Lin, S. G. Johnson, P. R. Villeneuve, J. D. Joannopoulos, J. R. Wendt, G. A. Vawter, W. Zubrzycki, H. Hou, and A. Alleman, *Nature (London)* **407**, 983 (2000).
- ³A. A. Erchak, D. J. Ripin, S. Fan, P. Rakich, J. D. Joannopoulos, E. P. Ippen, G. S. Petrich, and L. A. Kolodziejski, *Appl. Phys. Lett.* **78**, 563 (2001).
- ⁴S. Noda, A. Chutinan, and M. Imada, *Nature (London)* **407**, 608 (2000).
- ⁵C. Ren, J. Tian, S. Feng, H. Tao, Y. Liu, K. Ren, Z. Li, B. Cheng, and D. Zhang, *Opt. Express* **14**, 10014 (2006).
- ⁶S. W. Leonard, J. P. Mondia, H. M. van Driel, O. Toader, S. John, K. Busch, A. Birner, U. Gosele, and V. Lehmann, *Phys. Rev. B* **61**, R2389 (2000).
- ⁷W. Jia, Y. Li, Y. Xi, P. Jiang, X. Xu, X. Liu, R. Fu, and J. Zi, *J. Phys.: Condens. Matter* **15**, 6731 (2003).
- ⁸K. Yoshino, Y. Kawagishi, M. Ozaki, and A. Kose, *Jpn. J. Appl. Phys., Part 2* **38**, L786 (1999).
- ⁹Ch. Schuller, F. Klopff, J. P. Reithmaier, M. Kamp, and A. Forchel, *Appl. Phys. Lett.* **82**, 2767 (2003).
- ¹⁰G. Alagappan, X. W. Sun, P. Shum, M. B. Yu, and M. T. Doan, *J. Opt. Soc. Am. B* **23**, 159 (2006).
- ¹¹I. D. Villar, I. R. Matias, F. J. Arregui, and R. O. Claus, *Opt. Express* **11**, 430 (2003).
- ¹²Y. Ha, Y.-C. Yang, J.-E. Kim, H. Y. Park, C.-S. Kee, H. Lim, and J.-C. Lee, *Appl. Phys. Lett.* **79**, 15 (2001).
- ¹³H. F. Taylor, *J. Lightwave Technol.* **17**, 1875 (1999).
- ¹⁴E. H. Turner, *Appl. Phys. Lett.* **8**, 303 (1966).
- ¹⁵S. Okamura, Y. Mochiduki, H. Motohara, and T. Shiosaki, *Integr. Ferroelectr.* **69**, 303 (2005).
- ¹⁶B. Li, J. Zhou, Q. Li, L. T. Li, and Z. L. Gui, *J. Am. Ceram. Soc.* **86**, 867 (2003).
- ¹⁷B. Li, J. Zhou, L. T. Li, X. J. Wang, X. H. Liu, and J. Zi, *Appl. Phys. Lett.* **83**, 4704 (2003).
- ¹⁸J. W. Li, F. Duerwer, C. Gao, H. Chang, X. D. Xiang, and Y. L. Lu, *Appl. Phys. Lett.* **76**, 769 (2000).
- ¹⁹D. Y. Wang, H. L. W. Chan, and C. L. Choy, *Appl. Opt.* **45**, 1972 (2006).
- ²⁰D. Y. Wang, J. Wang, H. L. W. Chan, and C. L. Choy, *J. Appl. Phys.* **101**, 043515 (2007).
- ²¹E. Bormashenko, R. Pogreb, O. Stanevsky, Y. Bormashenko, Y. Socol, and O. Gendelman, *Polym. Adv. Technol.* **16**, 299 (2005).
- ²²X. K. Hong, G. J. Hu, J. Chen, J. H. Chu, N. Dai, and H. Z. Wu, *Appl. Phys. Lett.* **89**, 082902 (2006).
- ²³G. J. Hu, J. Chen, D. L. An, J. H. Chu, and N. Dai, *Appl. Phys. Lett.* **86**, 162905 (2005).
- ²⁴A. Urbas, R. Sharp, Y. Fink, E. L. Thomas, M. Xenidou, and L. J. Fetters, *Adv. Mater.* **12**, 812 (2000).
- ²⁵M. Plihal and A. A. Maradudin, *Phys. Rev. B* **44**, 8565 (1991).
- ²⁶O. Stenzel, *The Physics of Thin Film Optical Spectra An Introduction* (Springer, Berlin, 2005).
- ²⁷Y. H. Gao, H. Shen, J. H. Ma, J. Q. Xue, J. L. Sun, X. J. Meng, J. H. Chu, and P. N. Wang, *J. Appl. Phys.* **102**, 064106 (2007).
- ²⁸A. Boudrioua, J. C. Loulergue, E. Dogheche, and D. Remiens, *J. Appl. Phys.* **85**, 1780 (1999).
- ²⁹J. Li, M. H. Lu, L. Feng, X. P. Liu, and Y. F. Chen, *J. Appl. Phys.* **101**, 013516 (2007).
- ³⁰M. Schmidt, M. Eich, U. Huebner, and R. Boucher, *Appl. Phys. Lett.* **87**, 121110 (2005).